

Uncertainties and Sensitivity Analyses of ULOF and UTOP in Sodium-cooled Fast Reactor

R. Calabrese

ENEA, Nuclear Safety and Sustainability Division, Via Martiri di Monte Sole 4, I-40129
Bologna, Italy, rolando.calabrese@enea.it

ABSTRACT

In the frame of the OECD Nuclear Energy Agency (NEA) initiatives, the Expert Group on Innovative Fuel Elements (EGIFE) of the Working Party on Scientific Issues of Fuel Cycles (WPFC) has started a follow up of the benchmark on fuel performance codes. Phase II is focused on fast reactor cores loaded with either oxide or metal fuel. In particular, the participants will evaluate the behaviour of fuel pins during two accidental conditions: loss of flow and over power unprotected transients (ULOF, UTOP). In this exercise ENEA will use the TRANSURANUS fuel performance code. In these years the team of TRANSURANUS developers has devoted significant efforts to improve and refine models for fast reactor fuel pins. However, high burn-up, transient conditions, innovative cladding/fuel materials are all factors that contribute to increase uncertainties affecting predictions. Therefore, findings of best estimate calculations should be carefully considered and discussed in the light of each source of uncertainty. This paper presents an uncertainties and a sensitivity analysis of the transients proposed within the EGIFE benchmark. This analysis has been performed by applying the statistical module of TRANSURANUS which has been recently improved with additional capabilities.

1 INTRODUCTION

As mentioned in the abstract, the Expert Group on Innovative Elements (EGIFE) has proposed and organized a continuation of the benchmark on fuel performance codes [1]. Phase II will deal with fuel codes' simulations on loss of flow and over power unprotected transients (ULOF, UTOP) in fast reactors. ENEA will study the case of a reactor core loaded with MOX fuel. A second test case is proposed within the benchmark that is based on the use of metallic fuel. MOX fuel is clad with the 9Cr-Oxide Strengthened Steel (ODS). This alloy should be capable of meeting the ambitious requirements of innovative fast reactors. These systems are designed to deal with demanding irradiation conditions for the cladding: high temperature environment of around 700 °C and average burn-up of 150 GWd/t_{HM} with peak neutron doses as high as 250 dpa [2].

An example of fuel performance analysis of slow power transients in fast reactor is presented in [3]. This paper gives an extensive description of the models applied in calculations, mechanism of failure, and a detailed presentation of predictions during both base irradiation and transient [3]. Outcomes of the experiment presented in [3] confirm the role of fuel melting. During the experiment the onset of melting increased the cavity pressure, this in turn exacerbated PCMI leading to failure of the fuel pin [3]. An extensive database of slow power transients is presented and discussed in [4]. Main conclusion of this analysis addresses the importance of cavity pressurization that could be superimposed to PCMI especially for fuel pins with high values of smeared density. The experiments with pins characterized by

low values of smeared density show that the cavity pressurization is less important. In these experimental tests failure occurred with molten areas covering the majority of the fuel pellet [4]. Tsuboi et al. aiming at discussing the effect of fabrication uncertainties re-evaluated an experiment conducted in the CABRI facility [5]. They discuss each uncertain input in correlation with the quantities that are relevant for over power transients: gas retention at the end of pre-irradiation, porosity distribution, fuel and cladding deformation [5]. Herbreteau et al. have developed a tool for the evaluation of safety margins during power excursions [6]. In their modelling of fuel and cladding strains the authors identify as most relevant following contributions: thermal expansion, elastic and plastic strains. In case of melting the code has the capabilities for calculating the molten cavity pressure [6]. Analyses of ULOF and UTOP transients in sodium-cooled fast reactors are presented in [7,8]. However, the approach used in these works is based on a description of the whole plant and is not focused on fuel performance. This brief review has provided a series of indications regarding the role of relevant parameters during slow power excursions however, it has not suggested an assessed methodology for a statistical analysis of ULOF and UTOP in fast reactors.

This paper proposes a statistical analysis on uncertainties and sensitivity of unprotected transients. At this stage, uncertainties affecting fuel and cladding properties and relevant quantities such as linear heat rate and mass flow rate have been modelled and accounted for in calculations by means of the statistical module of TRANSURANUS [9].

2 STATISTICAL ANALYSIS METHODOLOGY

The TRANSURANUS code, since its first version (URANUS), has the capabilities required for conducting statistical analyses on fuel performance [10]. The approach used in this type of analyses has been based on a Monte-Carlo technique. At the time, sampling of random inputs could be carried out using Gaussian probability density functions (PDF). Additional types of probability density functions (uniform, log-normal, Cauchy) have been introduced in the code for a better modelling of random inputs. In parallel, number and types of random inputs have been increased. More than 70 variables that are relevant for fuel performance can be considered in a TRANSURANUS statistical analysis. This set of parameters can be grouped as follows:

- fuel, cladding, and coolant physical properties;
- input quantities depending on time (e.g., linear heat rate, mass flow rate, etc.);
- specific models (e.g., gap conductance, irradiation induced densification, diffusion coefficients, etc.);
- geometric quantities and plenum characteristics (fuel inner radius, cladding outer radius, etc.).

Uncertainties of random inputs are propagated to the outputs of interest. This data can be used to perform a quantitative evaluation of sensitivities. TRANSURANUS can calculate Pearson's correlation coefficients (PCC) and Spearman's rank correlation coefficients (SCC) for a large number of quantities. PCC provide an evaluation on the presence of a linear correlation between random variables under consideration; see Eq. 1.

$$PCC = \frac{\sum_{i=1}^n (x_i - \bar{x})(y_i - \bar{y})}{\sqrt{\sum_{i=1}^n (x_i - \bar{x})^2} \sqrt{\sum_{i=1}^n (y_i - \bar{y})^2}} \quad (1)$$

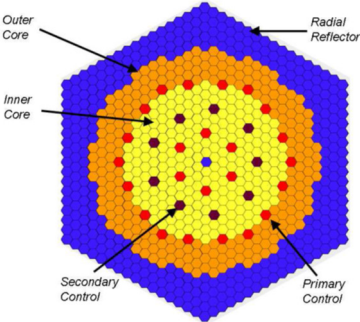
SCC use ranks in the place of numerical values. Correlation coefficients are calculated according to Eq. 1. This statistic gives indications about the existence of monotonic correlations between random variables. Uncertainties and correlation coefficients are

calculated as a function of time and axial position. Examples of uncertainties and sensitivity analyses performed on LOCA and RIA transients are presented in [11,12].

3 SODIUM-COOLED FAST REACTOR

The reactor core is loaded with MOX fuel and has a thermal power of 3600 MW_{th} [13]. The central region houses 225 subassemblies, while 228 subassemblies are sited in the outer zone. In addition, the reactor design is composed of 270 radial reflector subassemblies and 27 control subassemblies. Main specifications of the fuel subassembly and fuel pin are listed in Tab. 1 [13,14]. MOX fuel is clad with the 9Cr-ODS alloy [2,15]. Pins are arranged in a triangular lattice. Nominal inlet and outlet coolant temperature are 395 °C and 545 °C, respectively. The operating conditions of the inner zone that have been used in calculations are characterized by a peak linear heat rate of 41.1 kW/m and a peak fast neutron flux (> 0.1 MeV) of $1.91 \cdot 10^{15}$ n/cm²·s. These values do not vary throughout the irradiation cycle thanks to a reduced reactivity swing. Base irradiation is composed of 5 cycles of 410 EFPD/cycle.

Table 1: Layout of the core and geometrical specifications (cold and hot conditions)

	Fuel pin	Cold
	Fuel inner diameter (mm)	2.500
	Fuel outer diameter (mm)	9.430
	Clad inner diameter (mm)	9.730
	Clad outer diameter (mm)	10.730
	Upper plenum volume (mm ³)	7206.3
	Lower plenum volume (mm ³)	66176.8
	Fuel subassembly	Hot
	Length of subassembly (cm)	311.16
	Upper gas plenum (cm)	10.05
	Lower gas plenum (cm)	89.91
	Active core height (cm)	100.56
	Subassembly outer flat-to-flat (cm)	20.7468
	Number of fuel pins	271

4 DESCRIPTION OF CALCULATIONS

This paper presents a deterministic analysis of the base irradiation which is important as it determines the pre-transient conditions. Two unprotected transients have been simulated: an over power transient occurring at the beginning of cycle 1 and a loss of flow accident occurring at the end of cycle 5. During each transient a statistical analysis has been carried out. These analyses have been performed using the RESTART option of TRANSURANUS. ULOF and UTOP transients have been applied to a corner fuel pin of a subassembly sited in the inner zone. Operating conditions of this zone of the core are more demanding than in the outer zone. The 9Cr-ODS alloy is not comprised among the material options of the code, therefore, its correlations have been introduced for the purpose [2].

The TRANSURANUS modelling has been based on recommended options. Most relevant models are: OXIREN and PUREDII for oxygen and plutonium redistribution under irradiation [16,17]; relocation according to an empirical model for FBR [18]. Concerning densification, a model based on the work of Dienst et al. [19] and the data on pore migration by Olander [20] has been applied. The value of residual porosity at end of densification was set to 1%. Formation and closure of a central hole was accounted for. With regard to the mechanical

analysis, a visco-elastic treatment of creep in the fuel and an explicit treatment of creep in the cladding have been employed. Fission gas release modelling is based on a constant grain boundary saturation limit [21,22]. The fuel pin geometry has been described by means of 20 axial slices with a height of 0.05 m.

The use of an innovative cladding alloy is expected to introduce additional uncertainties in predictions. Besides this, the EGIFE is working on the preparation of a set of recommended properties for MOX. This initiative aims at reducing the scatter of codes' predictions due to the use of different models for fuel physical properties. Therefore, given a lack of an assessed methodology that has been mentioned in the introduction, the calculations presented here consider following types of uncertain inputs: fuel and cladding properties together with two variables important for the operating conditions: the linear heat rate and the mass flow rate of coolant. At this stage, all random inputs are characterized by a Gaussian PDF having a standard deviation of 5% and cut off set at 10%.

According to the indications of the literature, the outputs of interest are:

- fuel inner radius and gap width;
- fuel inner temperature;
- coolant temperature;
- clad average tangential stress.

Results at given times and axial positions are presented in following sections. Statistical calculations of TRANSURANUS are based on 1000 successful code runs.

5 PRE-TRANSIENT CONDITIONS

As aforementioned, two unprotected accidents are presented here: an over power transient occurring at the beginning of cycle 1 and a loss of flow accident at the end of cycle 5. Therefore, pre-transient conditions are quite different. In one case we have a fresh fuel in the other a fuel pin irradiated up to high burn-up. With regard to the initial conditions of the ULOF transient, a peak burn-up of 143600 MWd/t_{HM} and a corresponding fast neutron fluence of $0.34 \cdot 10^{+24}$ n/cm²·s are predicted at the end of base irradiation (slice 10 - PPN). The integral fission gas release at EOL is 63.5%. Fuel inner temperatures decrease due to restructuring occurring at BOL. An increase is noted due to fission gas release that is already significant at the end of cycle 1 (about 53%); see Fig. 1 (left). Closure of the gap between the fuel and the cladding occurring from the second cycle onwards plays a relevant role to limit the increase of fuel temperature: see Fig. 1 (right).

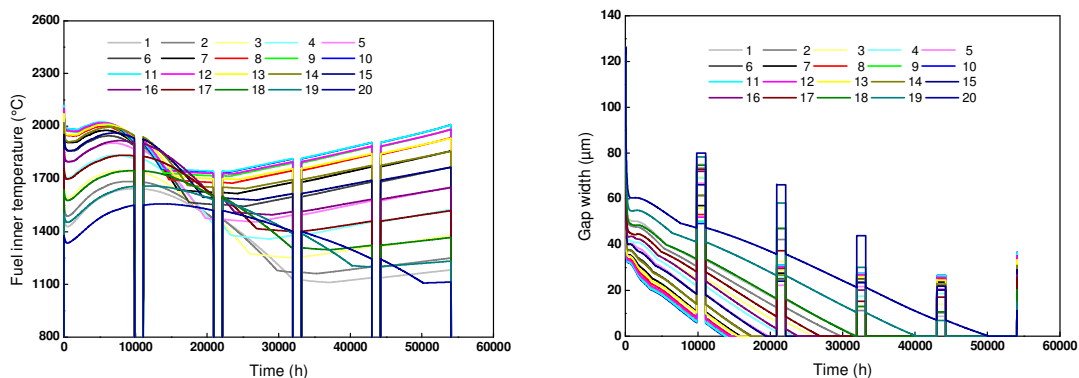


Figure 1: Fuel central temperature (left) and gap width (right) as a function of time

At EOL the gap is closed along the entire fuel stack. Fig. 2 (left) shows the decrease of the gap width due to fuel swelling. The permanent deformation of the cladding due to creep and swelling tends to increase the residual gap especially in the central region. The permanent tangential strain at O/M interface reaches a value of 1.13% at EOL (PPN). Values decrease to 0.28% for slice 1 and to 0.11 % for slice 20. The code does not model the formation of a JOG at high burn-up so that it is expected an overestimation of the permanent tangential strain. The fuel inner radius is smaller in the central region of the fuel column due to creep during PCMI; see Fig. 2 (right).

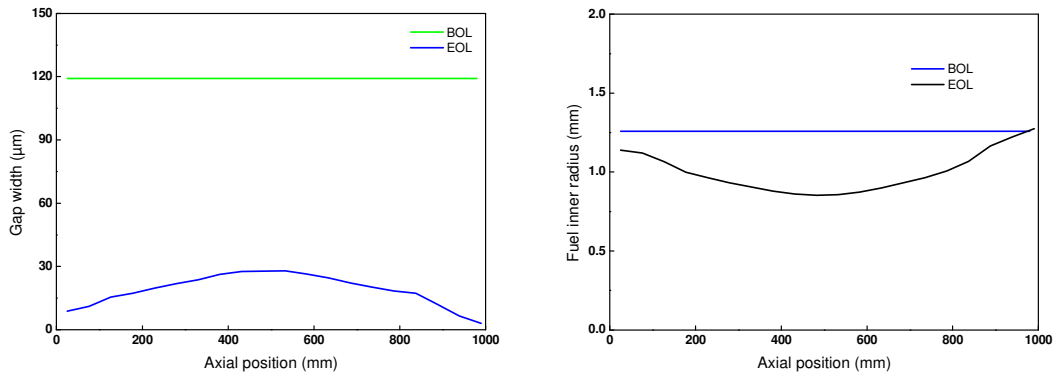


Figure 2: Gap width (left) and fuel inner radius (right) as a function of axial position (20 °C)

6 OVER POWER TRANSIENT (UTOP)

An overpower transient is applied at the beginning of cycle 1. The transient starts when the heat rate has reached its nominal value (41.1 kW/m at PPN). The first part of the transient (about 15 s) consists of a linear increase of power up to a level that is about 22% higher than nominal conditions. Thereafter, the heat rate is rather flat up to 300 s when transient ends: see Fig. 3 (left). During transient the coolant mass flow rate is maintained constant. The heat rate raw data was pre-processed by means of the *Fuel Rod Analysis ToolBox* [23] with a reduction in the number of time steps from 3000 to 234. The results of a deterministic run indicated that the gap remains open and that maximum temperatures are seen at the end of transient. Results of uncertainties analysis are presented in Fig. 3 (right) and Fig. 4 (left). They indicate a reduction in the margin to melting of about 124 °C as a consequence of the uncertainties considered in calculations.

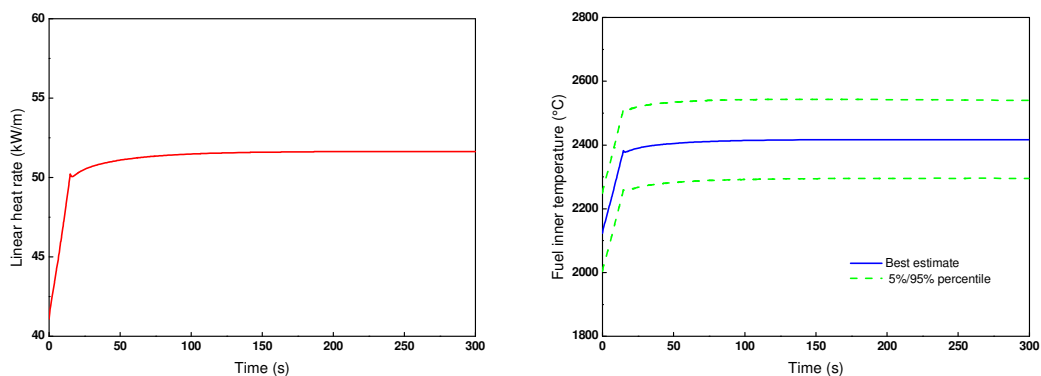


Figure 3: UTOP transient (left) and fuel inner temperature at PPN (right)

The Spearman's rank correlation coefficients shown in Fig 4 (right) confirm that the fuel inner temperature is strongly correlated with the fuel thermal conductivity while no evident correlation is seen with the other fuel properties. Low values of SCC indicate that no correlation is suggested between the fuel inner temperature and properties of the cladding (not shown). Results presented in Tab. 2 indicate that the uncertainties affecting the fuel inner temperature predictions are more significant than cladding and coolant temperature.

Some evaluations on geometric quantities are reported in Tab. 3. Highest uncertainties affect the gap width. These results confirm that the gap remains open during transient. Low uncertainties affect the inner and outer fuel radius. These calculations may indicate that porosity migration could cause an increase of the fuel inner radius not seen in the best estimate results.

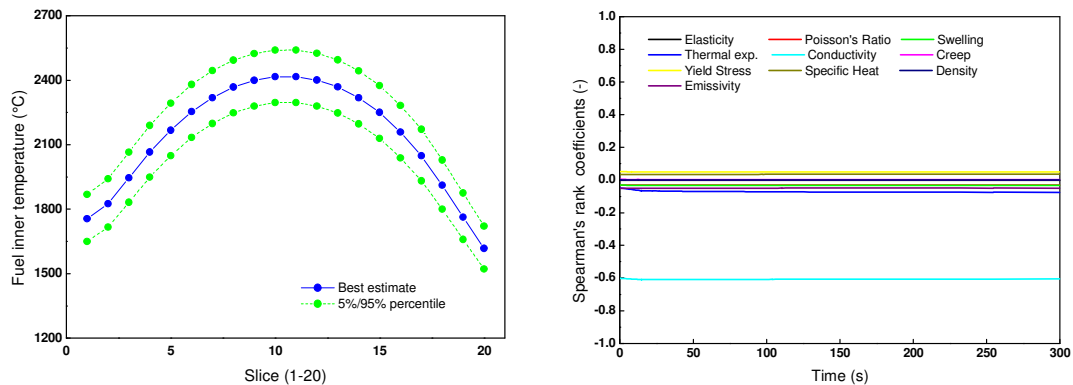


Figure 4: Axial profile of fuel inner temperature at EOL (left); correlation coefficients (SCC) of inner temperature at PPN vs. fuel properties (right)

Table 2: Uncertainties of peak values (axial position in brackets) of temperatures at EOL

Temperature	Best estimate (°C)	Standard deviation (°C)	5% percentile (°C)	95% percentile (°C)	Relative std. dev. (%)
fuel, inner (10)	2416.23	74.60	2295.63	2540.35	3.09
clad, inner (20)	605.01	9.55	589.19	620.85	1.58
coolant (20)	584.19	8.50	569.98	598.09	1.46

Table 3: Uncertainties of geometric quantities at 20 s (first row) and 300 s (second row)

slice 10 - PPN	Best estimate	Standard deviation	5% percentile	95% percentile	Relative std. dev. (%)
fuel inner (mm)	1.286	0.001	1.284	1.289	0.11
	1.291	0.005	1.286	1.301	0.38
fuel outer (mm)	4.850	0.006	4.840	4.860	0.12
	4.851	0.006	4.842	4.861	0.11
gap width (μm)	46.105	4.522	38.236	53.463	9.81
	44.478	4.423	36.805	51.765	9.94

7 LOSS OF FLOW TRANSIENT (ULOF)

An unprotected loss of flow is postulated at the end of cycle 5. Coolant mass flow rate at end of transient is 25.2% of the nominal value. During transient reactivity feedbacks lead to

a linear decrease of heat rate by about 13%. Calculations end at 30 s before the onset of sodium boiling occurring at 32 s.

Results of a deterministic run suggested that during transient the gap between the fuel and the cladding remains closed confirming the presence of PCMI. An increase of the coolant and cladding temperature induces a decrease of the cladding yield stress, however, no plastic deformation of the cladding was predicted at EOL. Statistical runs have confirmed that the gap is closed during transient. Uncertainties of the fuel inner radius and fuel temperature at PPN together with coolant temperature (slice 20) are reported in Tab. 4. Uncertainties are fairly constant during the transient confirming the indications provided by the deterministic run. These results support the hypothesis that fuel creep deformation does not occur during the transient.

Table 4: Uncertainties of fuel pin quantities at 5 s (first row) and 30 s (second row)

	Best estimate	Standard deviation	5% percentile	95% percentile	Relative std. dev. (%)
fuel inner radius (mm)	0.846	0.001	0.843	0.848	0.155
	0.847	0.001	0.845	0.849	0.130
fuel inner temperature (°C)	2036.64	98.06	1889.74	2209.91	4.81
	2043.51	93.27	1898.26	2202.34	4.56
coolant temperature (°C)	620.75	14.20	598.28	644.59	2.29
	920.86	30.95	869.68	973.76	3.36

Concerning the onset of plastic deformation, we present the average tangential stress of slice 11 in Fig. 5 (left). This figure also shows the cladding yield stress according to the temperature presented in Fig. 5 (right). The temperature used for the evaluation of yield stress has been determined by averaging the 95% percentile of the cladding inner and outer temperatures at the same axial position. As shown in these figures, the yield stress crosses the 95% percentile of the average tangential stress suggesting the onset of plastic deformation in the second part of the transient. This behavior has been confirmed by the analysis of slices 11-16 with a peak of deformation occurring in slice 14 (0.158% - 95% percentile).

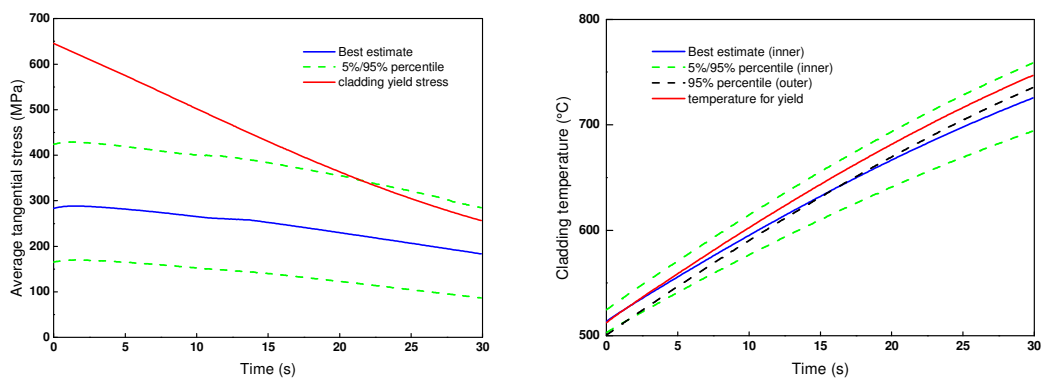


Figure 5: Average tangential stress and values of yield stress (left) calculated at the cladding temperature shown in the graph aside (slice 11) (right)

A sensitivity analysis of the cladding average tangential stress (slice 11) and average effective plastic strain (slice 14) is presented in Fig. 6 (left) and Fig. 6 (right). This analysis has confirmed that the thermal conductivity and thermal expansion of fuel are highly correlated with the two outputs under consideration. Correlation of cladding properties was less evident with values of SCC lower than 0.1 (not shown).

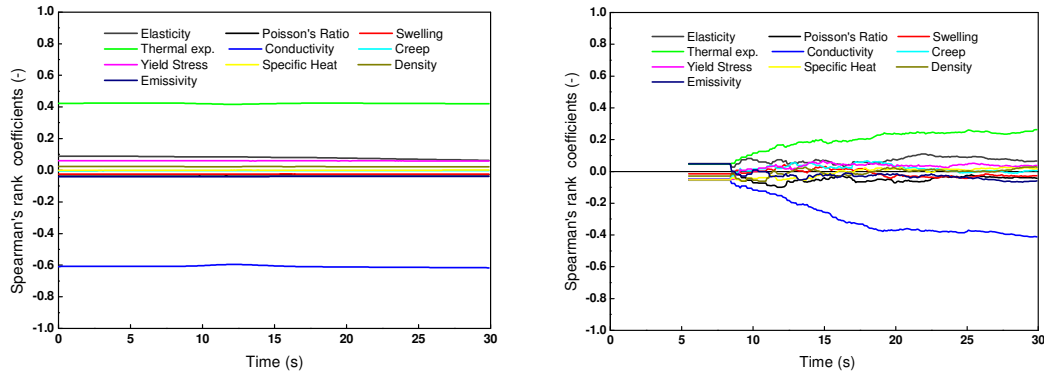


Figure 6: Evaluation of correlation coefficients (SCC) of tangential stress (slice 11) (left) and plastic deformation (slice 14) (right) vs. fuel properties

8 CONCLUSIONS

This paper presents some results of a statistical analysis conducted on two unprotected transients occurring in a sodium-cooled fast reactor loaded with MOX fuel. These transients have been proposed within the EGIFE benchmark Phase II. This analysis has been focused on the uncertainties of fuel and cladding material properties. Results presented here have been obtained by means of the TRANSURANUS code using its statistical module that has been recently improved and extended. If on the one hand, indications of deterministic runs have been largely confirmed, on the other hand, the statistical analysis has suggested that the occurrence of some processes not predicted in a deterministic run could affect the results. In particular porosity migration during fuel densification and onset of plastic deformation of the cladding have been outlined in our analysis. The sensitivity analysis has suggested that the thermal conductivity and thermal expansion of fuel are highly correlated with the outputs of interest. These preliminary results have confirmed the relevance of coupling best estimate with uncertainties for a careful testing of predictions.

REFERENCES

- [1] https://www.oecd-nea.org/science/wpfc/index_if.html.
- [2] T. Kaito, S. Mizuta, T. Uwaba, S. Ohtsuka, S. Ukai, 2005, “The Tentative Materials Strength Standard of ODS Ferritic Steel Claddings”, JNC TN9400 2005-015.
- [3] Y. Tsuboi, H. Endo, T. Ishizu, I. Tatewaki, H. Saito, H. Ninokata, 2012, “Analysis of fuel pin behavior under slow-ramp type transient overpower condition by using the fuel performance evaluation code FEMAXI-FBR”, Journal of Nuclear Science and Technology, 49:4, pp. 408-424.
- [4] Y. Fukano, Y. Onoda, I. Sato, J. Charpenel, 2009, “Fuel Pin Behavior under Slow-Ramp-type Transient-Overpower Conditions in the CABRI-FAST Experiments”, Journal of Nuclear Science and Technology, 46:11, pp. 1049-1058.
- [5] Y. Tsuboi, H. Endo, T. Ishizu, I. Tatewaki, H. Saito, H. Ninokata, 2012, “Sensitivity analysis of fuel pin failure performance under slow-ramp type transient overpower condition by using a fuel performance analysis code”, Journal of Nuclear Science and Technology, 49:10, pp. 975-987.
- [6] K. Herbreteau, N. Marie, F. Bertrand, J.-M. Seiler, P. Rubiolo, 2018, “Sodium-cooled fast reactor pin model for predicting pin failure during a power excursion”, Nuclear Engineering and Design, 335, pp. 279-290.

- [7] E.-E. Morris, W.-M. Nutt, 2011, “Uncertainty Analysis for Unprotected Accidents in Sodium-Cooled Fast Reactors”, *Journal of Nuclear Science and Technology*, 48:4, pp. 532-537.
- [8] M. Schikorr, E. Bubelis, B. Carlucci, J. Champigny, 2015, “Assessment of SFR reactor safety issues. Part I: Analysis of the unprotected ULOF, ULOHS and UTOP transients for the SFR (v2b-ST) reactor design and assessment of the efficiency of a passive safety system for prevention of severe accident”, *Nuclear Engineering and Design*, 85, pp. 249-262.
- [9] K. Lassmann, 1992, “TRANSURANUS: a fuel rod analysis code ready for use”, *Journal of Nuclear Materials*, 188, pp. 295-302.
- [10] K. Lassmann, C. O'Carroll, J. van de Laar, 1994, “Probabilistic fuel rod analyses using the TRANSURANUS code”, *Technical Committee Meeting on Water Reactor Fuel Element Modelling at High Burnup and Experimental Support*, International Atomic Energy Agency, Windermere, UK, 19-23 September, IAEA-TECDOC-957, 1997, pp. 497-506.
- [11] Z. Soti, A. Schubert, P. Van Uffelen, 2018, “Uncertainty and sensitivity analysis of nuclear fuel performance during a LOCA test case on the basis of the TRANSURANUS code”, *ANS Best Estimate Plus Uncertainty International Conference (BEPU 2018)*, Real Collegio, Lucca, Italy, May 13-19, p. BEPU2018-311.
- [12] A. Schubert, Z. Soti, P. Van Uffelen, 2018, “Extension of the TRANSURANUS Fuel Performance Code for Uncertainty/Sensitivity Analyses and its Application to Design-Bases Accidents” in *TOPFUEL 2018* 30 September - 04 October, Prague Czech Republic, paper A0067.
- [13] D. Blanchet, L. Buiron, N. Stauff, T.K. Kim, T. Taiwo, 2011, “AEN–WPRS Sodium Fast Reactor Core Definitions” (available in <https://www.oecd-nea.org/science/wprs/sfr-taskforce/>).
- [14] X. Du, Y. Zheng, L. Cao, H. Wu, 2018, “Transient analysis of MOX-3600 and MET-1000 sodium-cooled fast reactor using SARAX code system”, *Annals of Nuclear Energy*, 121, pp. 324–334.
- [15] S. Xu, Z. Zhou, W. Zheng, H. Jia, 2019, “Mechanical properties evaluation and plastic instabilities of Fe-9%Cr ODS steels”, *Fusion Engineering and Design* 149, p. 111335.
- [16] K. Lassmann, 1987, “The OXIREM Model for Redistribution of Oxygen in Nonstoichiometric Uranium-Plutonium Oxides”, *Journal of Nuclear Materials* 150, pp. 10-16.
- [17] V. Di Marcello, V.V. Rondinella, A. Schubert, J. van de Laar, P. Van Uffelen, 2014, “Modelling actinide redistribution in mixed oxide fuel for sodium fast reactors”, *Nuclear Energy*, 72, pp. 83-90.
- [18] T. Preusser, K. Lassmann, 1983, SMIRT 1983, Chicago paper C 4/3, “Current Status of the Transient Integral Fuel Element Performance Code URANUS”.
- [19] W. Dienst, I. Mueller-Lyda, H. Zimmermann, 1979, *International Conference on Fast Breeder Reactor Fuel Performance*, Monterey, California, 5-8 March, pp. 166.
- [20] D.R. Olander, 1979, “Fundamental aspects of nuclear reactor fuel elements”, *Technical Information Center - Energy Research and Development Administration*, University of California, Berkeley, TID-26711-P1.
- [21] K. Lassmann, H. Benk, 2000, “Numerical algorithms for intragranular fission gas release”, *Journal of Nuclear Materials*, 280(2), pp. 127-135.
- [22] K. Lassmann, 2000, “Numerical algorithms for intragranular diffusional fission gas release incorporated in the TRANSURANUS code”, *International Seminar on Fission Gas Behavior in Water Reactor Fuels*, Cadarache, France, 26-29 September, pp. 499-510.

- [23] K. Lassmann, A. Schubert, J. van de Laar, P. Van Uffelen, 2015, “The ‘Fuel Rod Analysis ToolBox’: A general program for preparing the input of a fuel rod performance code”, *Annals of Nuclear Energy*, 81, pp. 332–335.